Microgrooves on titanium surface affect peri-implant cell adhesion and soft tissue sealing; an *in vitro* and *in vivo* study

Hyo-Jung Lee[1,†], Jaden Lee[2,8,†], Jung-Tae Lee[1,3], Ji-Soo Hong[4,9], Bum-Soon Lim[5,9], Hee-Jung Park[6], Young-Kwang Kim[7], Tae-Il Kim[8,9*]

[1]Department of Periodontology, Section of Dentistry, Seoul National University Bundang Hospital, Seongnam, Korea

[2]Department of Oral Health Sciences, Medical University of South Carolina College of Dental Medicine, Charleston, SC, USA

[3]Department of Periodontics, Dankook University College of Dentistry Jukjeon Dental Hospital, Yongin, Korea

[4]Department of Oral Pathology, Seoul National University School of Dentistry, Seoul, Korea

[5]Department of Dental Biomaterials, Seoul National University School of Dentistry, Seoul, Korea.

[6]Department of Public Health Sciences, Korea University, Seoul, Korea

[7]Department of General Dentistry, Boston University School of Dental Medicine, Boston, MA, USA

[8]Department of Periodontology, Seoul National University School of Dentistry, Seoul, Korea

[9]Dental Research Institute, Seoul National University School of Dentistry, Seoul, Korea

pISSN 2093-2278
eISSN 2093-2286

JPIS Journal of Periodontal & Implant Science

Research Article

J Periodontal Implant Sci 2015;45:120-126
http://dx.doi.org/10.5051/jpis.2015.45.3.120

Received: Mar. 20, 2015
Accepted: May 25, 2015

*Correspondence:
Tae-Il Kim
Department of Periodontology, Seoul National University School of Dentistry, 101 Daehak-ro, Jongno-gu, Seoul 110-749, Korea
Email: periopf@snu.ac.kr
Tel: +82-2-2072-2642
Fax: +82-2-744-1349

†Hyo-Jung Lee and Jaden Lee contributed equally to this study.

Purpose: With the significance of stable adhesion of alveolar bone and peri-implant soft tissue on the surface of titanium for successful dental implantation procedure, the purpose of this study was to apply microgrooves on the titanium surface and investigate their effects on peri-implant cells and tissues.

Methods: Three types of commercially pure titanium discs were prepared; machined-surface discs (A), sandblasted, large-grit, acid-etched (SLA)-treated discs (B), SLA and microgroove-formed discs (C). After surface topography of the discs was examined by confocal laser scanning electron microscopy, water contact angle and surface energy were measured. Human gingival fibroblasts (hGFs) and murine osteoblastic cells (MC3T3-E1) were seeded onto the titanium discs for immunofluorescence assay of adhesion proteins. Commercially pure titanium implants with microgrooves on the coronal microthreads design were inserted into the edentulous mandible of beagle dogs. After 2 weeks and 6 weeks of implant insertion, the animal subjects were euthanized to confirm peri-implant tissue healing pattern in histologic specimens.

Results: Group C presented the lowest water contact angle (62.89 ± 5.66 θ), highest surface energy (45 ± 1.2 mN/m), and highest surface roughness (Ra = 22.351 ± 2.766 μm). The expression of adhesion molecules of hGFs and MC3T30E1 cells was prominent in group C. Titanium implants with microgrooves on the coronal portion showed firm adhesion to peri-implant soft tissue.

Conclusions: Microgrooves on the titanium surface promoted the adhesion of gingival fibroblasts and osteoblastic cells, as well as favorable peri-implant soft tissue sealing.

Keywords: Cell adhesion, Dental implants, Titanium, Wound healing.

INTRODUCTION

Titanium is used as a reliable biomaterial through dental implant procedure to treat edentulous areas. Osseointegration, a direct structural and functional binding reaction between bone and titanium, ensures stable dental implant fixation in the alveolar bone [1]. Crestal bone loss around titanium implant, however, has been reported with the presence of an inflammatory infiltrate in the titanium implant-surrounding gingival soft tissue [2]. Since

peri-implant soft tissue does not attach to the surface of titanium, it is vulnerable to bacterial invasion which often leads to peri-implant disease [3]. Therefore, tight soft tissue sealing around titanium implant is also regarded as important as osseointegration.

Several studies have been performed to promote peri-implant soft tissue attachment by physical and chemical modification of titanium surface. It was demonstrated that the soft tissue attachment was not influenced by the roughness of the titanium surface [4]. However, concave transmucosal-profiled titanium implants may promote connective tissue attachment around implants during the early healing phase [5]. In those studies, researchers modified the abutment or transmucosal area of titanium implants to investigate peri-implant soft tissue reactions.

As the actual morphology of alveolar ridge is not flat, it often occurs that not all surfaces of titanium implant fixtures are covered with the recipient bone in dental implant fixture installation procedure. In this context, successful outcome of dental implant treatment requires stable hard/soft tissue attachment to the titanium implant fixtures, while little has been known of the peri-implant soft tissue reaction on non-submerged coronal part of titanium implant fixtures.

In this study, we applied microgrooves on the titanium surface and investigated their effects on peri-implant soft tissue cells and tissues by *in vitro* and *in vivo* experiments.

MATERIALS AND METHODS

Titanium discs preparation

Commercially pure, grade 4 titanium discs (Dentium Co., Seoul, Korea) with 10 mm diameter and 2 mm thickness were divided into three groups as follows; machined-surface discs (A), sandblasted, large-grit, acid-etched (SLA)-treated discs (B), SLA-treated and microgroove (width × depth, 200 μm × 100 μm; distance between microgrooves, 50 μm)-formed discs (C). All samples were washed in an ultrasonic bath by using distilled water and stored in 100% ethanol at room temperature.

Surface characterization

Surface roughness was estimated using laser scanning confocal microscope (Zeiss LSM 5 Pascal, Carl Zeiss Inc., Oberkochen, Germany) with imaging software (Zeiss LSM Image Examiner, Carl Zeiss Inc.). The multi-argon laser emits light with a wavelength of 633 nm. This allows the calculation of the arithmetic mean of surface roughness from a mean plane in the sampling area (900 × 900 × 350 μm). To evaluate surface wettability, water contact angle was measured by sessile drop method at room temperature. A video camera with an image analyzer (Phoenix 300, Surface Electro Optics, Seoul, Korea) visualized the shape of the drop and provided the contact angle. Three probe liquids of different polarities were used: 1-bromonaphthalene, formamide, and deionized water. The volume of liquid drops was controlled using an instrument with a computerized interface and pictures of the drops were taken as soon as they landed on the surfaces using a video camera. Right and left contact angles of each drop were automatically averaged to give one contact angle per drop. Then, the surface free energy was calculated using three contact angle values from three different probe liquids according to the van Oss model. Each experiment was repeated 5 times for 3 specimens of each experimental group. The surface energy was calculated using the Owens–Wendt equation [6].

Immunofluorescence analysis

Human gingival fibroblasts (hGFs), purchased from ScienCell (Carlsbad, CA, USA), and murine osteoblastic MC3T3-E1 cells were seeded at 1×10^4 cells/well in a 24-well plate. After 24 hours cell culture, the cells were washed with PBS and fixed using 4% paraformaldehyde solution. The fixed cells were permeabilized with buffered 0.3% Triton X-100 at room temperature. The samples were blocked with 1% bovine serum albumin (BSA) for 1 hour. Actin (Abcam, Cambridge, MA, USA) was applied as the primary antibody and then reacted with fluorescein isothiocyanate (FITC)-conjugated secondary antibodies (Sigma, St. Louis, MO, USA). The samples were then reacted with 4,6-diamidino-2-phenylindole (DAPI) (Sigma) for visualizing the nuclei. All the labeled cells were examined using the Confocal Laser Scanning Microscope (FV300, Olympus, Center Valley, PA, USA) equipped with FITC - and DAPI - channel filter systems (Olympus).

Animal surgery

Four adult male beagle dogs (average age, 2 years; average weight, 13 kg) received dental prophylaxis for sustaining healthy periodontal conditions. Animal experiments were carried out in accordance with the Guidelines of the National Institute of Health (NIH) regarding the care and use of animals for experimental procedures and with the protocols approved by the Institutional Animal Care and Use Committee of Seoul National University (14-016-BA1402-147-007-01). Under general anesthesia by 2% xylazine hydrochloride (Rumpun, Bayer Korea, Seoul, Korea) with tiletamine hydro-chloride (Zoletil, Virbac, Ltd., Carros, France) and local anesthesia using 2% lidocaine hydrochloride with 1:100,000 epinephrine (Lidocaine, Huons, Seoul, Korea), mandibular 2nd, 3rd, and 4th premolars on both sides were extracted. After 12 weeks of healing under the same anesthetic conditions as those of the tooth extraction procedure, SLA-treated titanium implants (diameter × length; 3.1 mm × 9mm), with microgrooves (width × depth, 200 μm × 100 μm; distance between microgrooves, 50 μm) in the coronal portion, were installed according to the guideline of manufacturer (Dentium, co, Seoul, Korea). The experiment was performed with a balanced block design in which different groups of implants were randomly placed in each extraction socket according to the Latin block experimental design; group A, implants installed with 1 mm exposure of coronal microgroove portion; group B, implants installed with 2 mm exposure of coronal microgroove portion (Fig. 1). After connecting healing abutments and suturing, antibiotics (Cefazolin, 30 mg/kg, Chong Kun Dang Pharmaceutical Co., Seoul, Korea) were

dx.doi.org/10.5051/jpis.2015.45.3.120

JPIS Journal of Periodontal & Implant Science

intramuscularly injected with soft diet feeding. After 2 and 6 weeks, the animals were euthanized for mandibular block sections.

Histologic specimen preparation

In preparation for histologic specimens, the mandibular blocks were dehydrated in 70-100% ethanol, embedded in methacrylate (Technovit 7200 VCL, Kulzer, Wehrheim, Germany), and sectioned in the mesio-distal plane by using a diamond saw (Exakt, Apparatebau, Norderstedt, Germany). From all the block sections, the central four sections were reduced to a final thickness of 50 μm and stained by hematoxylin and eosin. The specimens were histologically analyzed under an optical microscope (Leica DM 2500, Leica Microsystems, Wetzlar, Germany).

Histometric analysis

Digital images were captured and a computer-based image analysis system (Image-Pro Plus, Media Cybernetic, Silver Spring, MD, USA) was used to quantify the findings. The soft tissue contact ratio was measured along the continuous line of soft tissue attachment within 3 cycles of micro-grooved pitch from the coronal part of fixture.

Statistical analysis

All statistical analyses were conducted using the statistical program (SPSS Inc., Chicago, IL, USA). One-way analysis of variance (ANOVA) was used to compare the mean values of the contact angle and surface energy. Mann–Whitney U test was used to compare the mean values from the results of histometry. The threshold for statistical significance was set at $P<0.05$.

RESULTS

Each group of titanium discs showed unique surface characteristics (Fig. 2). The machined-surface presented the lowest value of average roughness (Ra = 0.537 ± 0.051 μm), root mean square roughness (Rq = 0.681 ± 0.059 μm) and valley depth (Rz = 2.169 ± 0.239

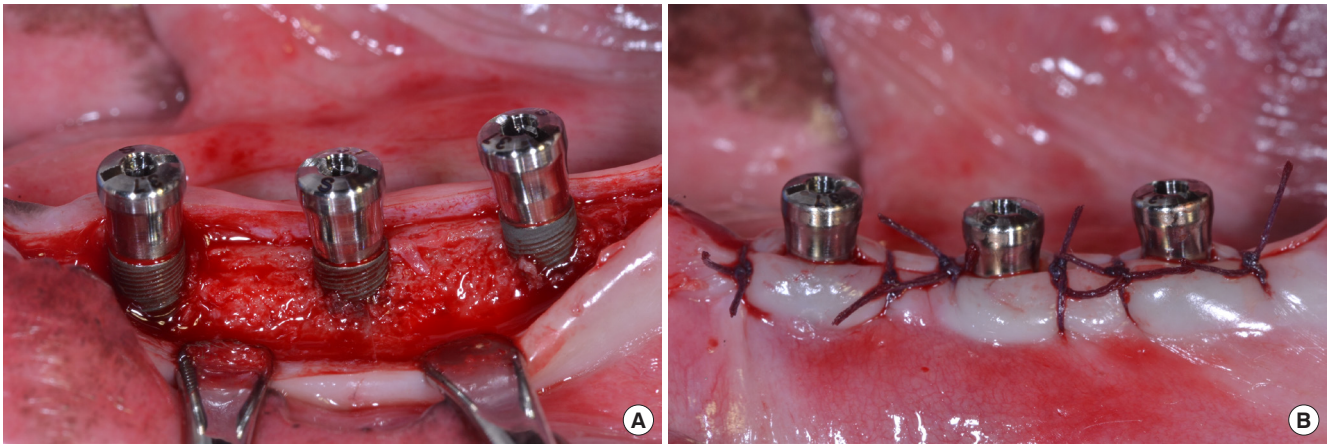

Figure 1. Sandblasted, large-grit, acid-etched (SLA)-treated titanium implants with microgrooves in the coronal portion were installed in the edentulous mandible of experimental animal (A), and gingival flaps were sutured (B).

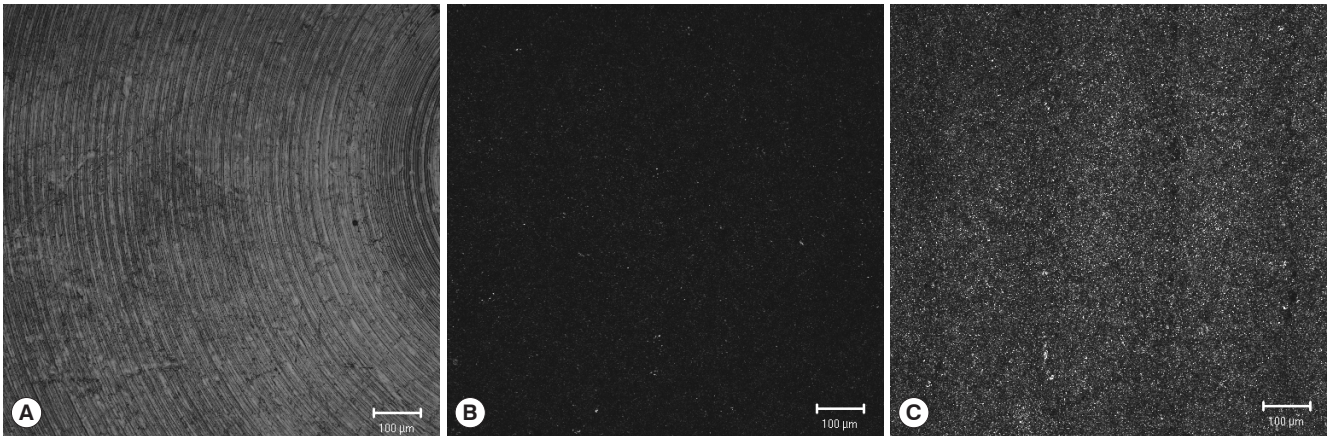

Figure 2. Laser scanning confocal microscopic images of titanium discs. A, machined-surface discs; B, sandblasted, large-grit, acid-etched (SLA)-treated discs; C, SLA-treated and microgroove-formed discs. Bar = 100 μm.

μm), while the SLA-treated group showed increased values (Ra = 1.285 ± 0.025 μm, Rq = 1.759 ± 0.037 μm, Rz = 6.652 ± 0.797 μm). The SLA-treated and microgroove-formed discs showed the highest values in the average roughness, root mean square roughness, and valley depth, which were 22.351 ± 2.766 μm, 25.202 ± 2.472 μm, and 46.161 ± 4.904 μm, respectively (Table 1).

Table 1. Surface roughness parameters of titanium discs using laser scanning confocal microscopy.

	A	B	C
Ra (μm)	0.537 ± 0.051	1.285 ± 0.025	22.351 ± 2.766
Rq (μm)	0.681 ± 0.059	1.759 ± 0.037	25.202 ± 2.472
Rz (μm)	2.169 ± 0.239	6.652 ± 0.797	46.161 ± 4.904

A, machined-surface discs; B, sandblasted, large-grit, acid-etched (SLA)-treated discs; C, SLA-treated and microgroove-formed discs.
Ra, roughness average; Rq, root mean square roughness; Rz, valley depth.

Multiple-comparison results of water contact angle analysis revealed that microgrooves and subsequent SLA treatment significantly increased hydrophilicity of titanium comparing to single SLA treatment procedure ($P<0.05$) (Fig. 3). Moreover, The SLA-treated and microgroove-formed discs showed the highest surface energy value, while there were no significant differences compared to SLA-treated group (Fig. 4).

Immunofluorescence analysis for hGFs and MC3T3-E1 cells adhesion revealed prominent expression of actin filaments and nuclei on the surface of the SLA-treated and microgroove-formed discs (Figs. 5 and 6).

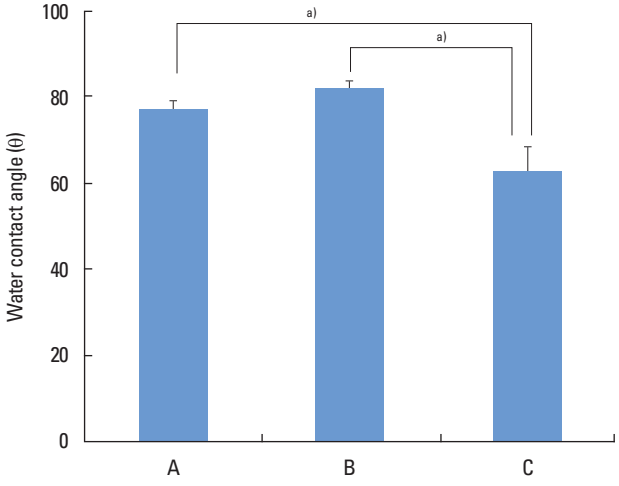

Figure 3. Water contact angle determination on titanium discs. A, machined-surface discs; B, sandblasted, large-grit, acid-etched (SLA)-treated discs; C, SLA-treated and microgroove-formed discs. [a]$P<0.05$, using the One-way ANOVA.

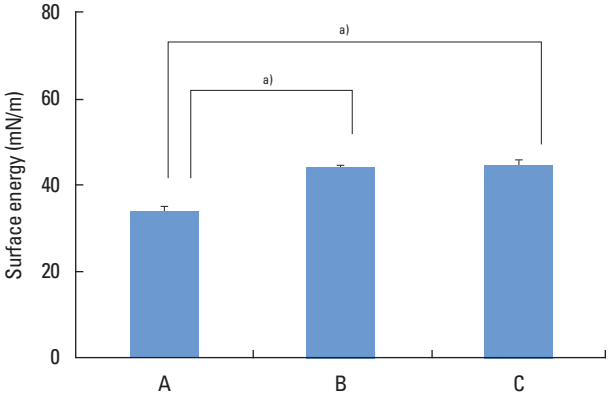

Figure 4. Surface energy determination on titanium discs. A, machined-surface discs; B, sandblasted, large-grit, acid-etched (SLA)-treated discs; C, SLA-treated and microgroove-formed discs. [a]$P<0.05$, using the One-way ANOVA.

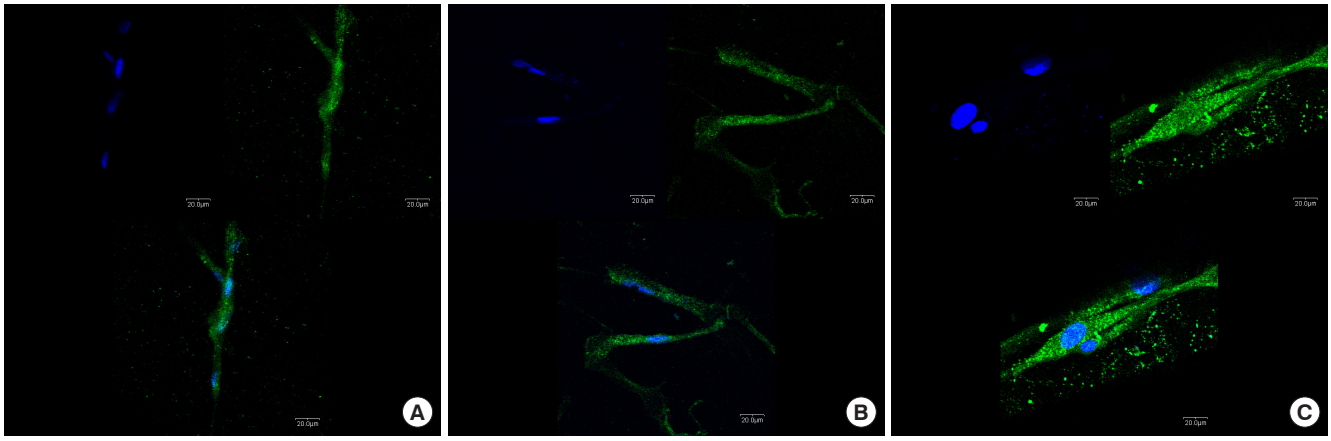

Figure 5. Immunofluorescence images showing actin filaments (green) and nuclei (blue) of human gingival fibroblasts on titanium discs for 24 hours. Prominent cell adhesion was induced in group C. A, machined-surface discs; B, sandblasted, large-grit, acid-etched (SLA)-treated discs; C, SLA-treated and microgroove-formed discs. Bar = 20 μm.

dx.doi.org/10.5051/jpis.2015.45.3.120

JPIS Journal of Periodontal & Implant Science

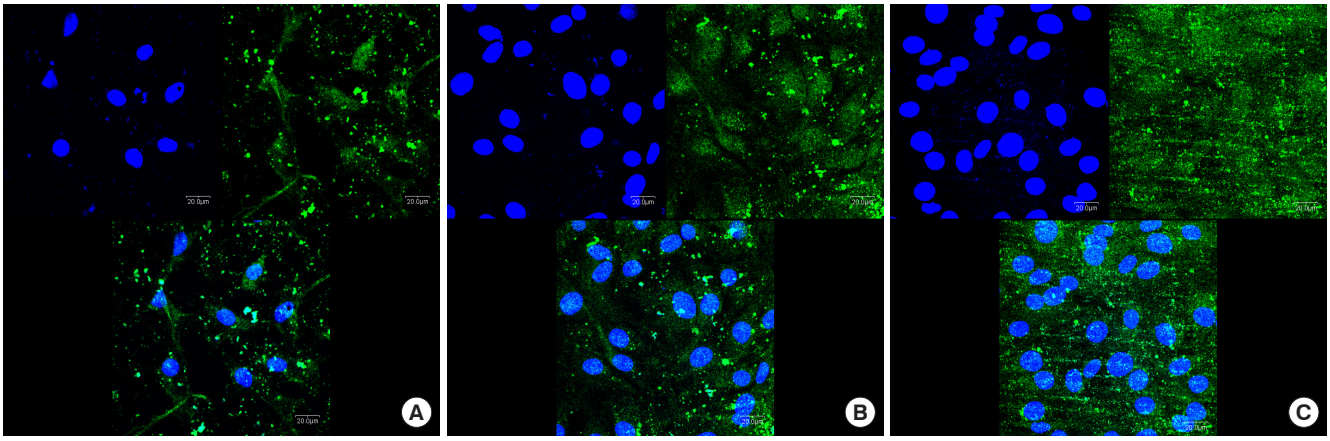

Figure 6. Immunofluorescence images showing actin filaments (green) and nuclei (blue) of murine osteoblastic cell line (MC3T3-E1) on titanium discs for 24 hours. Prominent cell adhesion was induced in group C. A, machined-surface discs; B, sandblasted, large-grit, acid-etched (SLA)-treated discs; C, SLA-treated and microgroove-formed discs. Bar = 20 μm.

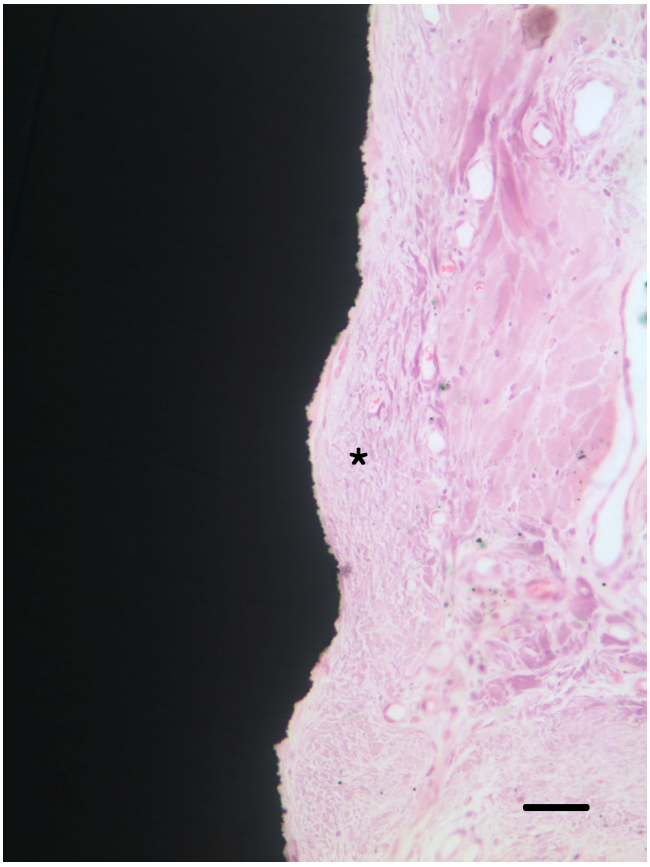

Figure 7. Light microscopic photographs at 2 weeks after implant installation. Peri-implant soft tissue was tightly attached to SLA-treated microgroove portion of titanium implant surface. Dense collagen fibers with circular alignment around microgroove surface were found (asterisk). Bar = 50 μm.

None of the implants, installed in the mandible of experimental animals, failed without any serious complications. There were no

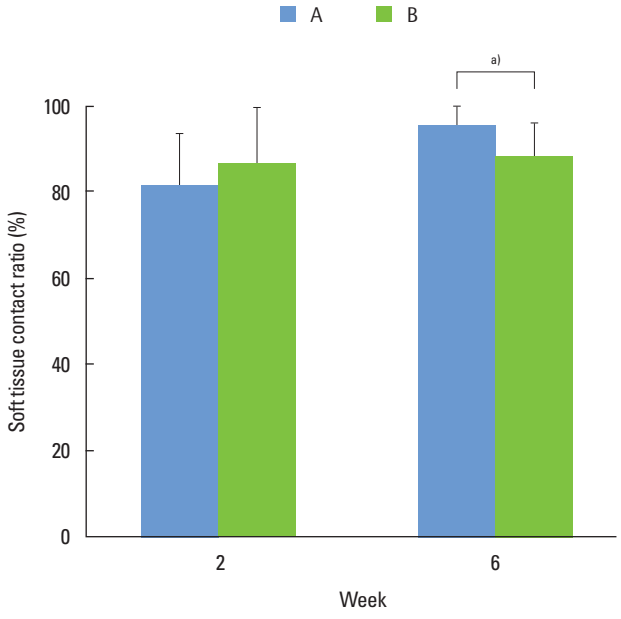

Figure 8. Soft tissue contact ratio determination on SLA-treated microgroove portion of titanium implant surface. A, implants installed with 1 mm exposure of coronal microgroove portion; B, implants installed with 2 mm exposure of coronal microgroove portion. [a] $P < 0.05$, using the Mann–Whitney U test.

signs of abscess, infection, or any wound dehiscence throughout the experimental period. Histological samples showed direct soft tissue contact with the surface of microgroove portion of the implants. Under microscopic examination, tight sealing of soft tissue contact was well established as most of the collagen fibers ran parallel to the surface of microgroove. Collagen fibers showed additional running patterns around microgroove surface, including a circular direction (Fig. 7).

At 2 weeks after implant insertion, the soft tissue contact ratio in group A was lower than that of group B on the area of microgroove

implant surface (Fig. 8). There was no statistically significant difference between two groups at 2 weeks ($P>0.05$). However, at 6 weeks after implant installation, both groups showed increased soft tissue contact ratio comparing to the values of 2 weeks after surgery. The soft tissue contact ratio of group A was higher than that of group B with a statistically significance ($P<0.05$)

DISCUSSION

Our present study showed that the SLA-treated and microgroove-formed titanium discs pertained the roughest surface characteristics and maintained the highest hydrophilicity comparing to the machined-surface or SLA-treated groups. Furthermore, the SLA-treated and microgroove-formed titanium surface promoted the adhesion of gingival fibroblasts and osteoblastic cell *in vitro*, and peri-implant soft tissue healing *in vivo* to a greater extent.

It has been reported that the roughness and surface energy of titanium surface affect the cellular adhesion [7-11]. In this present study, the dimensions of microgrooves (200 μm width and 100 μm depth) were determined considering the mean size of hGFs (100 μm). Our *in vitro* study results revealed that microgrooves with subsequent SLA treatment on titanium surface increased hydrophilicity significantly and promoted the adhesion of peri-implant soft tissue cells, i.e., gingival fibroblasts and osteoblastic cells. Based on these *in vitro* results, we performed animal experiments using titanium implants which had microgrooves with subsequent SLA treatment in their coronal portion.

Previous report demonstrated that the alveolar crestal bone level was located up to 2 mm below the implant-abutment junction [2]. In order to simulate this condition, we prepared titanium implants, which have microgrooves with subsequent SLA treatment in the coronal 2 mm portion, and intentionally positioned them with 1 mm or 2 mm coronal exposure to the peri-implant soft tissue. In the present study, connective tissue with abundant fibroblasts accompanying a few vessels surrounded exposed microgroove portion, which corresponds to previous reports on peri-implant soft tissue healing [5,12,13]. While peri-implant soft tissue contact to the microgroove portion was increased in a time-dependent manner after implant installation surgery, 2 mm coronal exposure group showed significantly lower soft tissue contact ratio than that of 1 mm coronal exposure group at 6 weeks after surgery. This phenomenon might be a possible explanation as to why peri-implant soft tissue is vulnerable to bacterial invasion, often leading to peri-implant disease, which was addressed previously [3, 14-16]. The soft tissue attachment to dental implants differs from that of natural teeth in the orientation of the connective tissue attachment. In teeth, an attachment apparatus with Sharpey's fibers is found embedded in the cementum and covering the root surface at an oblique angle, while the implants have firm bundles of connective tissue fibers running parallel to the implant surface [17]. Our present findings were in agreement with this observational report. Considering the present results of soft tissue contact ratio measurement, we can deduct that more coronal exposure of implant fixtures leads to less soft tissue contact to implant, which may allow inflammatory infiltrate.

From a clinical viewpoint, with alveolar ridge not always being flat, it often occurs that not all coronal surfaces of titanium implant fixtures are covered with the recipient alveolar bone in dental implant fixture installation procedure. Thus, if the coronal surface of implant fixtures facilitates soft tissue contact, it can promote tight soft tissue sealing which is important to resist possible bacterial intrusion.

In this study, as the SLA-treated and microgroove-formed titanium surface also enhanced osteoblastic adhesion, it would be expected to promote alveolar bone contact if this surface was submerged in alveolar bone. Therefore, it is possible that the SLA-treated microgroove in the coronal portion of titanium implant may promote tight peri-implant soft tissue sealing together with osseointegration which is essential to the maintenance of dental implants. The determination of long-term *in vivo* response of peri-implant tissues may provide further evidence for the benefit of SLA-treated microgroove structures on the reliable dental implantation.

CONFLICT OF INTEREST

No potential conflict of interest relevant to this article was reported.

ACKNOWLEDGEMENTS

This research was supported by Seoul National University (Grant number: 860-20140001) and the International Research & Development Program of the National Research Foundation of Korea (NRF) funded by the Ministry of Science, ICT & Future Planning (Grant number: 2014K1A3A1A21001365).

ORCID

Hyo-Jung Lee *http://orcid.org/0000-0002-0439-7389*
Jaden Lee *http://orcid.org/0000-0001-6937-9416*
Jung-Tae Lee *http://orcid.org/0000-0001-5383-3004*
Ji-Soo Hong *http://orcid.org/0000-0001-5698-0894*
Bum-Soon Lim *http://orcid.org/0000-0003-3112-0227*
Hee-Jung Park *http://orcid.org/0000-0002-6789-9247*
Young-Kwang Kim *http://orcid.org/0000-0002-1984-206X*
Tae-Il Kim *http://orcid.org/0000-0003-4087-8021*

REFERENCES

1. Brånemark PI, Adell R, Albrektsson T, Lekholm U, Lundkvist S, Rockler B. Osseointegrated titanium fixtures in the treatment of edentulousness. Biomaterials 1983;4:25-8.
2. Hermann JS, Buser D, Schenk RK, Higginbottom FL, Cochran DL. Biologic width around titanium implants. A physiologically formed

and stable dimension over time. Clin Oral Implants Res 2000;11:1-11.
3. Geurs NC, Vassilopoulos PJ, Reddy MS. Soft tissue considerations in implant site development. Oral Maxillofac Surg Clin North Am 2010;22:387-405, vi-vii.
4. Abrahamsson I, Zitzmann NU, Berglundh T, Linder E, Wennerberg A, Lindhe J. The mucosal attachment to titanium implants with different surface characteristics: an experimental study in dogs. J Clin Periodontol 2002;29:448-55.
5. Huh JB, Rheu GB, Kim YS, Jeong CM, Lee JY, Shin SW. Influence of Implant transmucosal design on early peri-implant tissue responses in beagle dogs. Clin Oral Implants Res 2014;25:962-8.
6. Owens DK, Wendt RC. Estimation of surface free energy of polymers. J Appl Polym Sci 1969;13:1741-7.
7. Bächle M, Kohal RJ. A systematic review of the influence of different titanium surfaces on proliferation, differentiation and protein synthesis of osteoblast-like MG63 cells. Clin Oral Implants Res 2004;15:683-92.
8. Cooper LF, Zhou Y, Takebe J, Guo J, Abron A, Holmén A, et al. Fluoride modification effects on osteoblast behavior and bone formation at TiO2 grit-blasted c.p. titanium endosseous implants. Biomaterials 2006;27:926-36.
9. Kim MJ, Choi MU, Kim CW. Activation of phospholipase D1 by surface roughness of titanium in MG63 osteoblast-like cell. Biomaterials 2006;27:5502-11.
10. Marinucci L, Balloni S, Becchetti E, Belcastro S, Guerra M, Calvitti M, et al. Effect of titanium surface roughness on human osteoblast proliferation and gene expression in vitro. Int J Oral Maxillofac Implants 2006;21:719-25.
11. Sader MS, Balduino A, Soares GD, Borojevic R. Effect of three distinct treatments of titanium surface on osteoblast attachment, proliferation, and differentiation. Clin Oral Implants Res 2005;16:667-75.
12. Cochran DL, Hermann JS, Schenk RK, Higginbottom FL, Buser D. Biologic width around titanium implants. A histometric analysis of the implanto-gingival junction around unloaded and loaded nonsubmerged implants in the canine mandible. J Periodontol 1997;68:186-98.
13. Ruggeri A, Franchi M, Marini N, Trisi P, Piatelli A. Supracrestal circular collagen fiber network around osseointegrated nonsubmerged titanium implants. Clin Oral Implants Res 1992;3:169-75.
14. Broggini N, McManus LM, Hermann JS, Medina R, Schenk RK, Buser D, et al. Peri-implant inflammation defined by the implant-abutment interface. J Dent Res 2006;85:473-8.
15. Chehroudi B, Gould TR, Brunette DM. The role of connective tissue in inhibiting epithelial downgrowth on titanium-coated percutaneous implants. J Biomed Mater Res 1992;26:493-515.
16. Linkevicius T, Apse P. Biologic width around implants. An evidence-based review. Stomatologija 2008;10:27-35.
17. Gargiulo AW, Wentz FM, Orban B. Dimensions and relations of dentogingival junction in humans. J Periodontol 1961;32:261-7.